Published in final edited form as:
Magn Reson Med. 2011 May ; 65(5): 1297–1304. doi:10.1002/mrm.22723.

Fast Measurement of Blood T_1 in the Human Jugular Vein at 3 Tesla

Qin Qin[1,2], **John J. Strouse**[3], and **Peter C.M. van Zijl**[1,2,4]

[1]The Russell H. Morgan Department of Radiology and Radiological Science, Division of MR Research, The Johns Hopkins University School of Medicine, Baltimore, MD USA

[2]F.M. Kirby Center for Functional Brain Imaging, Kennedy Krieger Institute, Baltimore, MD USA

[3]Division of Pediatric Hematology, The Johns Hopkins University School of Medicine, Baltimore, MD USA

[4]Department of Biophysics and Biophysical Chemistry, The Johns Hopkins University School of Medicine, MD USA

Abstract

Current T_1 values for blood at 3T largely came from *in vitro* studies on animal blood or freshly drawn human blood. Measurement of blood T_1 *in vivo* could provide more specific information, e.g. for individuals with abnormal blood composition. Here, blood T_1 at 3T was measured rapidly (< 1min) in the internal jugular vein using a fast inversion-recovery technique in which multiple inversion time can be acquired rapidly due to constant refreshing of blood. Multi-shot EPI acquisition with flow compensation yielded high resolution images with minimum partial volume effect. Results showed T_1 = 1852 ± 104 ms among 24 healthy adults, a value higher than for bovine blood phantoms (1584 ms at Hct of 42%). A second finding was that of a significant difference ($P < 0.01$) between men and women, namely T_1 = 1780 ± 89 ms (n = 12) and T_1 = 1924 ± 58 ms (n = 12), respectively. This difference in normal subjects is tentatively explained by the difference in Hct between genders. Interestingly, however, studies done on sickle cell anemia patients with much lower Hct (23 ± 3%, n = 10) revealed similar venous blood T_1 = 1924 ± 82 ms, indicating other possible physical influences affecting blood T_1.

Keywords

in vivo blood T_1; inversion recovery; internal jugular vein; sickle cell anemia

Introduction

Knowledge of the absolute value of the longitudinal relaxation time (T_1) of blood is important for many quantitative MRI applications, including determination of cerebral blood flow (CBF) using arterial spin labeling (ASL) (1–4), calculation of the inversion time (TI) in vascular space occupancy (VASO)-dependent fMRI (5), and estimation of kinetic parameters (permeability and volume of distribution) in dynamic contrast-enhanced MRI (6).

Corresponding Author: Qin Qin or Peter C.M. van Zijl, Johns Hopkins University School of Medicine, Dept. of Radiology, 217 Traylor Bldg, 720 Rutland Ave, Baltimore, MD, 21205, qin@mri.jhu.edu or pvanzijl@mri.jhu.edu, Tel: 443-923-9511, Fax: 443-923-9505.

We have previously studied the T_1 of bovine blood at 3T using an *in vitro* circulation system under physiological conditions. This has the advantage of allowing measurement of T_1 as a function of hematocrit (Hct), oxygenation, and temperature (7). Similar to studies at lower fields (8–10), increased Hct and reduced temperature cause a reduction in blood T_1. Contrary to lower field, T_1 was slightly higher in arterial than in venous blood.

Measurements in physiological phantoms on animal or human blood are useful to show trends and find approximate T_1 values, but are unlikely to be identical to *in vivo* conditions due to several issues, including the need to add an anticoagulant (salt or heparin) and the formation of methemoglobin (MetHb) (11), which is more paramagnetic than deoxygenated hemoglobin. On the other hand, measurement of T_1 *in vivo* is complicated by the small size of microvascular blood vessels, the rapid flow of blood in larger vessels, and the variation in Hct between different types of blood vessels.

T_1 measurements on static spins using conventional inversion recovery (IR) are known to be reliable but lengthy, because data at only one TI is acquired per TR. The total measurement time is thus proportional to TR times the number of TIs (N_{TI}). The Look-Locker sequence (12) is a popular fast T_1 mapping technique that utilizes several small-flip-angle excitation pulses in one TR, which consequently sacrifices signal-to-noise ratio (SNR). However, T_1 measurement on fast flowing spins can be much more efficient. In large vessels, the in-flowing blood in the imaging slice does not experience the previous slice-selective excitation pulses. Data with multiple TIs can thus be acquired during a single TR. Therefore, the total duration for blood T_1 measurement does not need to be proportional to N_{TI}.

This idea has previously been demonstrated in renal arteries and veins for evaluating kidney extraction fractions (13,14). Recently, it was applied to measure T_1 in the posterior sagittal sinus (PSS) (15,16). Here we apply this approach to the internal jugular vein (IJV), which has the advantage of 1) allowing a much larger region of interest (ROI) and thus reduced partial volume effect with the static tissues; 2) minimizing the possibility that blood spins excited at the rest of the imaging slice at earlier TIs to drain through the ROI later, affecting the simple inversion recovery model.

Methods

Pulse Sequence

In Figure 1, the pulse sequence diagram for measuring T_1 in the flowing blood (13,14,16) is described. It is composed of a non-selective (NS) inversion pulse followed by an initial waiting time TI(1) and series of N_{TI} slice-selective (SS) 90° excitation pulses separated by a short time interval (ΔTI). It is assumed that all spins entering the imaging slice have experienced the inversion pulse, i.e. the transmit coil should be sufficiently large and the overall blood flow over arteries, microvessels, and veins sufficiently slow. This can be achieved for the brain when using body coil excitation and using the fact that the transit time from carotids to jugulars is about 5 – 10 s (17). When ΔTI is longer than a threshold determined by the slice thickness (THK) and through-plane flow velocity (v), $\Delta TI > THK/v$, the spins in the imaging slice will have been replenished by incoming ones that have experienced the NS inversion, but none of the previous SS excitations. Thus, these spins will be excited by the n^{th} SS pulse at inversion time ($TI(n) = TI(1) + (n - 1) \times \Delta TI$, $n = 1, 2, \ldots N_{TI}$). EPI-compatible first-order flow compensation (FC) gradients are used to reduce the phase loss caused by through-plane flow (18). For each gradient-echo EPI readout train (ACQ), using SENSE and multi-shot (N_{shots}) acquisition, only a fraction of *k*-space is sampled to shorten the echo time to minimize image distortion and flow-based spin loss. The same fractions of the *k*-space are sampled with different TIs after each inversion. Using a rapid series of excitation pulses, static spins will be saturated and show little background

signal. It is worth noting that the proposed sequence without the NS inversion pulse is essentially a 2D Time-Of-Flight (TOF) MRA technique (19), with its short TR the same as ΔTI here.

Data acquisition

All experiments were performed on a 3T Philips Achieva scanner (Philips Medical Systems, Best, The Netherlands) using the body coil for transmission and an 8-channel head coil for reception. 24 healthy adult volunteers (age: 35 ± 11 yrs; range: 24 – 63 yrs; 12 females and 12 males), 10 sickle cell anemia patients (age: 11 ± 2 yrs; range: 8 – 15 yrs; 5 females and 5 males) and 8 sibling controls (age: 12 ± 2 yrs, range: 9 – 14 yrs; 4 females and 4 males) were enrolled, all of who provided informed written consent (and assent for children) in accordance with local Institutional Review Board. Several volunteers were studied for parameter optimization.

As part of scan planning, a phase contrast MRA (PCA) survey image was acquired in the coronal plane to visualize the location of IJVs and other major neck vessels, including Internal Carotid Arteries (ICA), External Carotid Arteries (ECA), and Vertebral Arteries (VA). Subsequently, a sagittal PCA survey image was acquired on the dominant IJV. Both PCA survey scans used a 50 mm slab, TR/TE = 20/5.8ms, FOV = 250 × 250 mm^2, and a scan matrix of 256 × 128 (acquisition time: 20s for 2 averages). Then, phase contrast velocity measurements were performed on a 5 mm axial slice, positioned perpendicular to the targeted IJV about 15 mm below the superior bulb (Figs. 2a, b, c). This location was chosen for the large cross-sectional area of the IJV. Acquisition parameters: TR/TE = 15/9ms, 5 dynamics, FOV = 128 × 128 mm^2, acquisition matrix = 128 × 128 (reconstruction 256 × 256). The total acquisition duration was about 30 sec. For some scans of healthy adult subjects, a comparison study was conducted using gating by a Peripheral Pulse Unit (PPU) triggered with 15 phases per RR period, taking 1.5 min per average. The encoding velocity was set to be 40 cm/s for both of these quantitative flow scans.

For the IJV blood T_1 measurements, the experimental parameters were: FOV = 200 × 150 mm^2, acquisition matrix = 192 × 132, with left-right being the phase encoding direction. In-plane resolution after reconstruction was 0.78 × 0.78 mm^2. Since T_2^* of venous blood at 3T is about 20 ms (20) and the field inhomogeneity in this region is challenging due to tissue-air susceptibility difference, it is essential to have a short echo time (TE) to reduce signal loss and a short acquisition window to minimize image distortion. Also, one wants to minimize the distance over which spins flow in and out of the slice, which, when large, may affect signal quantification. The acquisition window for each subset of *k*-space (EPI factor (k_y lines) = 11) was slightly less than 20 ms. When including flow compensation (FC) and acquiring symmetric with respect to the readout train, TE = 15 ms. The full *k*-space at each TI was acquired with a 6-segment gradient echo EPI (N_{shots} = 6), with SENSE acceleration factor = 2. Adiabatic NS 180° inversion was performed using a hyperbolic secant pulse (21) of length 10 ms, peak power 13.5 μT, and bandwidth 1250 Hz. After inversion pulse and a spoiling gradient, the first acquisition was taken at TI(1) = 50 ms (shorter delay caused some eddy current artifacts) and the rest of acquisitions were taken at an interval ΔTI = 200 ms. Using N_{TI} = 50 acquisitions, TR was 9850 ms (≈ 10 s) for the 6 shots, leading to a total acquisition time of about 1 min.

To acquire proper inversion recovery curves from the flowing blood, it is crucial to invert all blood within body transmit coil (brain + neck and upper torso) before it drains through the IJV. Although the adiabatic 180° pulse used for inversion is expected to be insensitive to B_1 inhomogeneity, it will only function above the adiabatic RF power threshold (B_1) and within its bandwidth. The current bandwidth for inversion was 1250 Hz, which may make the inversion profile sensitive to B_0-inhomogeneity and thus to shimming. To properly setup the

scan, it is therefore essential to shim on the whole volume within the transmit coil and not only on the local slice acquired for acquisition. The effect of such partially non-selective inversion was therefore examined for different areas of the brain (top, middle, and bottom, all above the IJVs) by using the same NS 180° pulse and either adjusting both first and second order shims locally (around excitation slice only) or only 1st order shims locally following a global shim. Four subjects with left and right IJVs similar in orientation and sizes were chosen to first inspect the correspondence of measured blood T_1s from the two vessels. The same T_1 results are expected from the left and right IJVs of the same subject.

To determine an appropriate TR value and slice thickness, 6 volunteers were scanned with TR = 5, 7.5, and 10 s, using N_{TI} = 25, 37, and 49, and total acquisition times of 30, 45, and 60 s, respectively. Both 5 mm and 10 mm slice thickness were used for each TR, while all other imaging parameters were kept the same.

For the rest of the study, TR = 10 s and a slice thickness of 5 mm were used on an extended total of 24 healthy adult subjects (12 females, age: 37 ± 12 yrs, range: 24 – 62 yrs; 12 males, age: 33 ± 10 yrs, range: 24 – 63 yrs).

In a separate group of subjects recruited for a sickle cell study, individual Hct of both patients and sibling controls were measured: 10 sickle cell patients (5 females, age: 11 ± 1 yrs, range: 10 – 13 yrs, Hct: 23 ± 4%; 5 males, age: 10 ± 3 yrs, range: 8 – 15 yrs, Hct: 24 ± 3%) and 8 sibling controls (4 females, age: 11 ± 2 yrs, range: 9 – 13 yrs, Hct: 37 ± 2%; 4 males, age: 13 ± 3 yrs, range: 9 – 14 yrs, Hct: 40 ± 4%). Motion artifacts were sometimes observed with children right after the acquisition. Another data set would be obtained immediately to replace the corrupted data, after instructing the young subjects to stay still.

Data Analysis

Matlab 7.0 (MathWorks, Inc., Natick, MA, USA) was used for data processing. A ROI at the targeted IJV was manually drawn from the image acquired at the longest inversion time, $TI(N_{TI})$. The selected ROI was transferred to all other images in the set of N_{TI} images. All the images obtained at each TI with the ROI depicted were quickly reviewed to identify any shift of the ROI during the acquisition. Selected ROIs consistently covered the IJV throughout the TIs in each data set and no obvious shift was observed.

Within the selected ROI, the signal intensities (after magnitude processing) of each pixel were fitted as a function of TI using a 3-parameter model:

$$S(TI) = \left| S_0 \left(1 - 2\alpha e^{-TI/T_1} + e^{-TR/T_1} \right) \right| \quad [1]$$

The initial magnitude S_0, the inversion degree α, and the blood T_1 were fitted using the nonlinear-least-square algorithm of Matlab. The inversion degree was always restricted to be less than 1.0 and was found to be between 0.95 and 1.0 from all the fitting results. For individual measurements, the standard errors of the estimated T_1s fitted from ROI-based mean values are reported. For a group of measurements, the mean and standard deviation (sd) of the averaged T_1s over all subjects are calculated.

Results

Figs. 2a–c show typical imaging slice positions for the blood velocity measurement at the IJV, as chosen based on the scout images of anatomy and angiography. In an anatomical image of the chosen slice (Fig. 2d) significant asymmetry in the size of the IJVs is observed, as previously described (22). A quantitative velocity map (in cm/s) measured using phase contrast angiography is shown in Fig. 2e. Compared to the carotids (bright), the jugulars

(dark) have larger cross-section areas and flow slower with opposite direction. The dark regions inside the carotids are from aliasing due to the local blood velocity exceeding the encoding velocity, 40 cm/s in this study. In some scans, the averaged velocities from the ROIs of the dominant IJVs were compared between flow measurements with PPU triggering (1.5 min) and without (0.5 min). Results observed during the 15 phases of an R-R interval triggered by PPU showed some pulsation effects and ranged from 5 cm/s to 35 cm/s at different cardiac phases (similar with results in a Doppler ultrasound study (23)). These had the same average velocities as when measured using 5 dynamics without PPU triggering (Figure 2f). The velocity measurement without PPU triggering was therefore used on the remaining subjects. Average blood velocities in the IJVs were comparable for adult men and women, 16 ± 4 cm/s and 16 ± 3 cm/s, respectively. Sickle cell patients presented faster flow velocity in the IJVs (31 ± 4 cm/s) compared to sibling controls (23 ± 7 cm/s) (two-tailed Student *t*-test: P = 0.03).

The data in Fig. 3 show the effect of incorrect inversion on the T_1 measurements, Figs. 3e and 3f show the T_1 recovery curves when using higher order shimming on the local slice and when using global higher order shimming and only first order shimming locally, respectively. There is a clear left/right difference in Fig. 3e and both left and right T_1 values are much lower than in Fig. 3f. The reason is that when shimming locally with higher orders, the field adjustment may be totally off for other parts of the brain, moving the water proton frequency in such regions outside the bandwidth of the adiabatic inversion pulse. This effect is illustrated anatomically in Fig. 3c. When shimming globally with higher orders and followed by local adjustment with only linear shims, the inversion image looks much better (Fig. 3d). These results make sense because the success of the T_1 approach is dependent on the correctness of the assumption that all spins participating have experienced proper inversion. As the measurement is done over a period of 5 – 10 s, this means that most spins in the coil volume have to be inverted.

Table 1 shows the averaged blood T_1s of 6 subjects for three repeated measurements, when varying TR (5 s, 7.5 s, 10 s) and slice thickness (5 mm, 10 mm). With the same TR and THK, the three repeated measurements over 60 min period did not differ more than 100 ms (max-min). This variation could be due to physiological status of each subject (e.g. drinking of water before the experiment) (24) or measurement error. The results were fairly consistent among $3 \times 2 \times 3 = 18$ T_1s for each of 6 subjects being less than 3.5% (sd/mean). The ranges of the measurements for each individual were all less than 200 ms (max-min).

The individual blood T_1s measured for 24 healthy adults using TR = 10 s and 5 mm slice thickness are listed in Table 2. Significant differences in T_1 values (two-tailed Student *t*-test: $P < 0.01$) were observed between female subjects ($T_{1,\,IJV} = 1924 \pm 58$ ms, n = 12) and male subjects ($T_{1,\,IJV} = 1780 \pm 89$ ms, n = 12). The averaged blood T_1 of all 24 subjects was 1852 ± 104 ms.

For sickle cell patients (Hct = 23 ± 3%, n = 10), the averaged $T_{1,\,IJV}$ was 1924 ± 58 ms, in the range of those values of the sibling controls (females: $T_{1,\,IJV} = 1986 \pm 70$ ms, n = 4; males: $T_{1,\,IJV} = 1848 \pm 66$ ms, n = 4), and no significant difference between genders was found (P = 0.66), as opposed to the sibling controls (P = 0.02).

Discussion

It is shown that blood water T_1 in the internal jugular veins can be determined efficiently *in vivo* using an approach in which water spins in the upper torso and brain are inverted using a body coil, followed by rapid measurement of the blood signal recovery (every 200 ms) as a function of time after inversion while using 90° slice excitation pulses. The latter was

possible by using the inflow of fresh blood into the slice, in a manner similar to that previously demonstrated for the kidney (13,14) and the sagittal sinus (15,16). The jugular vein is actually quite optimal for this determination because of both its relatively large cross-sectional area (compared to the ICA) and fast through-plane flow velocity (compared to the sagittal sinus). Due to the relatively straight path of this vein, as compared to the sagittal sinus, it is also possible to use a large slice thickness. Finally, the background signal is efficiently saturated due to the rapid succession of 90° pulses. Even when some partial volume effects occur between tissue and blood, this will cause the same relative blood signal loss for each inversion time point and thus not contribute to the fitted T_1.

The results in Table 2 show that the T_1 values measured *in vivo*, 1924 ± 58 ms in 12 women and 1780 ± 89 ms in 12 men, are about 10–20% longer than previously measured (1584 ms) for typical Hct (42%) and oxygenation (60–69%) using *in vitro* bovine blood under physiological conditions (pH, temperature) (7). Bovine blood was used before because it is readily available and has similar physiological properties as human blood (25). However, the numbers given in this report are very close to a recent work measuring *in vitro* human blood at 3T (1932 ± 85 ms (26)) and two recent *in vivo* fast measurements on PSS (1862 ± 105 ms in 4 females and 1755 ± 126 ms in 4 males respectively (15), and 1717 ± 39 ms in total of 3 females and 4 males (16)). In another study of the field dependence of *in vivo* tissue T_1, blood T_1s were well fitted by an empirical function $1.315(B0)^{0.34}$ for B0 field between 0.2T to 7T (27), which gives blood T_1 = 1911 ms at 3T, also very close to our results. As such, it seems that these longer *in vivo* human T_1 values may be more appropriate to use for ASL and VASO experiments than our previous *in vitro* bovine blood numbers.

Technical Considerations

The validity of the approach is based on the correctness of several assumptions. The first is that all water spins are properly inverted by the non-selective adiabatic 180° pulse. This seems easy when using a body coil for excitation, but it was shown that care has to be taken to properly shim the body volume contained within the excitation coil, especially the brain, to assure that all resonance frequencies are within the bandwidth of the inversion pulse. Such global shimming can employ higher order shims, while the use of higher order shims on just the measurement slice should be avoided as such local shimming can cause large changes in the field remote from the slice, as demonstrated in Fig. 3.

The transit time of water through the human brain has been measured using ultrasound bolus tracking (17). Defining the global Cerebral Circulation Time (CCT) as the transit delay time between blood passing through the ICA and the ipsilateral IJV, Schreiber et al. (17) found CCT to be about 5.3 ~ 10.1s in normal adults, which is on the order of magnitude of the inversion times used. So most spins within the large coil volume will contribute (also those exchanged from tissue). Therefore, with our approach and depending on TR, the magnetization of blood will be either fully-relaxed (TR = 10s) or in steady-state (at shorter TR values). With longer TR, some noninverted blood may arrive at the IJV ROI at the later TIs, when the inverted blood are also close to fully recovered; with shorter TR, some blood may experience two inversion pulses and their magnetization would differ from the single inversion model. It is important to realize that this may vary in disease. For instance, patients with cerebral arteriovenous malformation are expected to have much shorter CCT (~ 1.5 s) due to a high arteriovenous shunt volume (17). In our approach, the maximum length of TI that can be used basically depends on the availability of inverted spins, which would be much shorter for such patients.

The second essential assumption for this T_1 approach to be correct is that the blood signals sampled at each TI are not affected by any of the slice-selective excitation pulses of the preceding TI points. This might not hold true in two scenarios: a. if there were remaining

blood within the coil volume that has not flowed out of the ROI during ΔTI. As we used the head coil and we waited 200ms between sample points, we do not expect this to be a problem. b, if some blood in another part of the imaging slice would be excited, circulate through the cerebral vascular network, and then drained through the ROI at a later acquisition time. Both effects would shorten the measured blood T_1. Notice that when using only a slice through the PSS for the T_1 measurement, the frontal sagittal sinus or other big veins in the same imaging slice might be repeatedly excited and eventually drain through the occipital sagittal sinus. This may explain the slightly shorter T_1s reported in two recent studies using the same technique on the PSS (15,16).

The proposed method was carried out employing first-order flow compensation gradients before acquisition, which assumes constant flow velocity in IJV during the 20 ms subset *k*-space acquisition window. This seems to be a valid assumption, given the slow-changing pulsatile flow patterns of IJV, as observed in this study (Figure 2f, top). Another aspect of pulsatile flow is that the slower velocities at certain cardiac phases maybe below the threshold velocity to induce signal loss. Longer ΔTI or smaller slice thickness would be needed to mitigate this effect. For turbulent flow presented in some diseases, cardiac gating might be necessary to improve the accuracy of this method (28), with the penalty of longer acquisition time.

Our T_1 approach seems especially suitable for draining veins, but less for feeding arteries, which are refreshed at very high speed. However, if one can invert sufficient torso blood signal to be able to reach the sign reversal point in the recovery curve, it may be possible to estimate T_1 just based on the zero point. Sampling can be done at higher temporal resolution as the flow is high, but it has to be kept in mind that arterial T_2* is relatively long and that ΔTI can thus not be too short as signal excited in the slice will flow into the brain and may be detected by the receiver coil. Since arterial blood water T_1 was found to be only about 100 ms higher than venous blood water T_1 at 3T in phantoms (7), T_1 measured at IJV could be used to estimate the arterial value.

With the knowledge of the global CCT (> 5 s) and jugular blood velocity (> 5 cm/s), TR = 10 s, ΔTI = 200 ms and slice thickness = 5 mm were chosen as optimal parameters for this method. The total measurement time of our sequence is the product of TR and number of shots. It currently takes up to 1 min (TR: 10 sec; $N_{shots} = 6$) to obtain the IR curves during each acquisition. This time can be reduced further when used for measuring T_1 after administering contrast agents.

Physiological Considerations

Relaxation times are easy to reduce due to experimental error or paramagnetic contamination, thus it is reasonable to conclude that the longer values found *in vivo* are probably correct, and it is necessary to analyze what may be causing the lower T_1 numbers in phantoms. T_1 is not very sensitive to oxygenation, so the 69% in the phantom versus about 60–64% *in vivo* is probably not relevant, especially because higher oxygenation would lengthen T_1 (7,9,10). T_1 is strongly dependent on Hct, as known from the experimentally determined dependence for the physiological phantom (7) at 3T:

$$1/\mathrm{T1}\ (\mathrm{s}^{-1}) = (0.83 \pm 0.07)\mathrm{Hct} + (0.28 \pm 0.03) \quad \text{venous blood} \qquad [2]$$

For a typical range of physiological Hct values between 36% and 46%, this gives T_1 numbers ranging from 1727 to 1511 ms, low compared to our human data. Thus, it seems that additional factors should be at play to cause the difference between bovine blood phantoms and human blood. The first that comes to mind is the sample preparation. When using *ex vivo* blood, an anti-coagulation agent has to be added, either heparin or sodium

citrate. Lu *et al*. (7), used 20 mM of the latter, which could potentially have some paramagnetic contamination. Another issue with *ex vivo* blood is the formation of MetHb (11), which is more paramagnetic than hemoglobin. Lu *et al*. kept the MetHb concentration below 1.5%, but this likely is much lower *in vivo* (0.64% for normal adults (29), and in another study (30), 0.3% in venous blood for people with sickle cell anemia, 0.24% for African-Americans without sickle cell disease). More studies will be needed to investigate the origin of this difference.

Another difference that occurs between phantoms and subjects is that *in vivo* blood water T_1 probably has a likely contribution from tissue T_1. The reason is that, for the longer inversion times, some venous blood water originates from tissue water that exchanged with blood water in the capillaries and is subsequently drained through the veins. Nevertheless such a contribution will only reduce T_1 and can thus not explain the increased values found. CSF also drains into venous blood through the arachnoid space and it does have much longer T_1 (4400 ms (27)), which could increase the measured jugular T_1. However, with a rather slow formation rate (0.35 ml/min (31)), less than 0.01 ml of water of CSF would drain into the total venous blood per second, which is too small to have an effect compared to a typical 30 ml venous blood volume (assuming a 75 Kg adult, 2% of brain mass and 2% of cerebral venous blood volume (31)).

Interestingly, a large (~ 10%), statistically significant ($P < 0.05$), difference was found between T_1 numbers measured in males and females. The female values are longer than the male ones, which may be due to a lower average Hct in women. The literature range for Hct in women versus men is 36% ~ 44% versus 41% ~ 50% (32). Bovine phantom data indicate that a difference in T_1 of 150 ms corresponds to about 0.075 difference in average Hct, which seems large but not unreasonable. Perhaps the Hct dependence of T_1 is stronger *in vivo* than *in vitro*, but this is hard to test unless direct sampling is done from the jugular veins of the volunteers studied.

The T_1s measured for participants with sickle cell anemia were not higher than those found for the sibling controls, which were comparable to the normal controls for men and women. This equivalence seems impossible when only considering Hct and this finding suggests influence of the variant sickle hemoglobin or cell shape on the T_1 relaxation mechanism. Sickled red blood cells might further enhance the longitudinal relaxation in whole blood, compared to the normal blood cells, thus canceling the slower relaxation effect due to the lower Hct.

Conclusions

We have shown that blood T_1 values can be measured efficiently *in vivo* (within 1 min) exploiting the inflow of fresh blood into the jugular veins. The resulting T_1 numbers were about 20% longer than those from physiological phantoms, which indicate a need to obtain more accurate values by performing measurements *in vivo* or by improving the experimental conditions for phantoms. The proposed fast method can be performed in combination with ASL, VASO, or dynamic Gd experiments for a subject-based blood T_1 determination, which is important based on the strong dependence of T_1 on Hct and the possibility of different T_1s in patients with blood abnormalities.

Acknowledgments

The authors are grateful to Joseph S. Gillen, Michael Schar (Philips), Jun Hua and Seth Smith for their suggestions in developing the pulse sequence. Ms. Terri Brawner, Ms. Kathleen Kahl, and Ms. Ivana Kusevic are thanked for experimental assistance. Rachel Han and Alan Huang helped with recruiting sickle cell patients. Dr. van Zijl is a paid lecturer for Philips Medical Systems. Dr. van Zijl is the inventor of technology that is licensed to Philips. This

arrangement has been approved by Johns Hopkins University in accordance with its conflict of interest policies. This research was made possible in part by a grant from the National Center for Research Resources (NCRR), a component of the National Institutes of Health (NIH). Its contents are solely the responsibility of the authors and do not necessarily represent the official view of NCRR or NIH.

Grant support from

NIH-NIBIB R01-EB002634 and NIH-NCRR P41-RR15241

5K23HL078819-04, Scholar Award from American Society of Hematology

References

1. Buxton RB, Frank LR, Wong EC, Siewert B, Warach S, Edelman RR. A general kinetic model for quantitative perfusion imaging with arterial spin labeling. Magnetic Resonance in Medicine. 1998; 40(3):383–396. [PubMed: 9727941]
2. Detre JA, Leigh JS, Williams DS, Koretsky AP. Perfusion Imaging. Magnetic Resonance in Medicine. 1992; 23(1):37–45. [PubMed: 1734182]
3. Zaharchuk G, Martin AJ, Dillon WP. Noninvasive imaging of quantitative cerebral blood flow changes during 100% oxygen inhalation using arterial spin-labeling MR imaging. AJNR Am J Neuroradiol. 2008; 29(4):663–667. [PubMed: 18397966]
4. Strouse JJ, Cox CS, Melhem ER, Lu H, Kraut MA, Razumovsky A, Yohay K, van Zijl PC, Casella JF. Inverse correlation between cerebral blood flow measured by continuous arterial spin-labeling (CASL) MRI and neurocognitive function in children with sickle cell anemia (SCA). Blood. 2006; 108(1):379–381. [PubMed: 16537809]
5. Lu H, Golay X, Pekar JJ, van Zijl PCM. Functional magnetic resonance Imaging based on changes in vascular space occupancy. Magnetic Resonance in Medicine. 2003; 50(2):263–274. [PubMed: 12876702]
6. Tofts PS, Kermode AG. Measurement of the Blood-Brain Barrier Permeability and Leakage Space Using Dynamic MR Imaging .1. Fundamental Concepts. Magnetic Resonance in Medicine. 1991; 17(2):357–367. [PubMed: 2062210]
7. Lu H, Clingman C, Golay X, van Zijl PCM. Determining the Longitudinal Relaxation Time (T1) of Blood at 3.0 Tesla. Magnetic Resonance in Medicine. 2004; 52(3):679–682. [PubMed: 15334591]
8. Silvennoinen MJ, Kettunen MI, Kauppinen RA. Effects of hematocrit and oxygen saturation level on blood spin-lattice relaxation. Magnetic Resonance in Medicine. 2003; 49(3):568–571. [PubMed: 12594761]
9. Bryant RG, Marill K, Blackmore C, Francis C. Magnetic-Relaxation in Blood and Blood-Clots. Magnetic Resonance in Medicine. 1990; 13(1):133–144. [PubMed: 2319929]
10. Brooks RA, Dichiro G. Magnetic-Resonance-Imaging of Stationary Blood - a Review. Medical Physics. 1987; 14(6):903–913. [PubMed: 3696078]
11. Farahani K, Saxton RE, Yoon HC, De Salles AAF, Black KL, Lufkin RB. MRI of thermally denatured blood: Methemoglobin formation and relaxation effects. Magnetic Resonance Imaging. 1999; 17(10):1489–1494. [PubMed: 10609997]
12. Look DC, Locker DR. Time saving in measurement of NMR and EPR relaxation times. Review of Scientific Instruments. 1970; 41:250–251.
13. Niendorf ER, Grist TM, Lee FT, Brazy PC, Santyr GE. Rapid in vivo measurement of single-kidney extraction fraction and glomerular filtration rate with MR imaging. Radiology. 1998; 206(3):791–798. [PubMed: 9494503]
14. Dumoulin CL, Buonocore MH, Opsahl LR, Katzberg RW, Darrow RD, Morris TW, Batey C. Noninvasive Measurement of Renal Hemodynamic Functions Using Gadolinium-Enhanced Magnetic-Resonance-Imaging. Magnetic Resonance in Medicine. 1994; 32(3):370–378. [PubMed: 7984069]
15. Wu WC, Jain V, Li C, Giannetta M, Hurt H, Wehrli FW, Wang J. In Vivo Venous Blood T1 Measurement Using Inversion Recovery True-FISP in Children and Adults. Magnetic Resonance in Medicine. 2010; 64(4):1140–1147. [PubMed: 20564586]

16. Varela M, Hajnal JV, Petersen ET, Golay X, Merchant N, Larkman DJ. A Method for Rapid *in vivo* Measurement of Blood T1. NMR In Biomedicine. 2010 in press.
17. Schreiber SJ, Kauert A, Doepp F, Valdueza JM. Measurement of global cerebral circulation time using power duplex echo-contrast bolus tracking. Cerebrovascular Diseases. 2003; 15(1–2):129–132. [PubMed: 12499722]
18. Butts K, Riederer SJ. Analysis of Flow Effects in Echo-Planar Imaging. Jmri-Journal of Magnetic Resonance Imaging. 1992; 2(3):285–293.
19. Keller PJ, Drayer BP, Fram EK, Williams KD, Dumoulin CL, Souza SP. Mr Angiography with Two-Dimensional Acquisition and 3-Dimensional Display - Work in Progress. Radiology. 1989; 173(2):527–532. [PubMed: 2798885]
20. Zhao JM, Clingman CS, Narvainen MJ, Kauppinen RA, van Zijl PCM. Oxygenation and Hematocrit dependence of transverse relaxation rates of blood at 3T. Magnetic Resonance in Medicine. 2007; 58(3):592–597. [PubMed: 17763354]
21. Silver MS, Joseph RI, Hoult DI. Highly Selective Pi/2 and Pi-Pulse Generation. Journal of Magnetic Resonance. 1984; 59(2):347–351.
22. Beards SC, Yule S, Kassner A, Jackson A. Anatomical variation of cerebral venous drainage: the theoretical effect on jugular bulb blood samples. Anaesthesia. 1998; 53(7):627–633. [PubMed: 9771169]
23. Pucheu A, Evans J, Thomas D, Scheuble C, Pucheu M. Doppler Ultrasonography of Normal Neck Veins. Journal of Clinical Ultrasound. 1994; 22(6):367–373. [PubMed: 8071454]
24. He X, Zhu M, Yablonskiy DA. Validation of oxygen extraction fraction measurement by qBOLD technique. Magnetic Resonance in Medicine. 2008; 60(4):882–888. [PubMed: 18816808]
25. Benga G, Borza T. Diffusional water permeability of mammalian red blood cells. Comparative Biochemistry and Physiology B-Biochemistry & Molecular Biology. 1995; 112(4):653–659.
26. Stanisz GJ, Odrobina EE, Pun J, Escaravage M, Graham SJ, Bronskill MJ, Henkelman RM. T-1, T-2 relaxation and magnetization transfer in tissue at 3T. Magnetic Resonance in Medicine. 2005; 54(3):507–512. [PubMed: 16086319]
27. Rooney WD, Johnson G, Li X, Cohen ER, Kim SG, Ugurbil K, Springer CS Jr. Magnetic field and tissue dependencies of human brain longitudinal 1H2O relaxation in vivo. Magn Reson Med. 2007; 57(2):308–318. [PubMed: 17260370]
28. Guo JY, Kim SE, Parker DL, Jeong EK, Zhang L, Roemer RB. Improved accuracy and consistency in T-1 measurement of flowing blood by using inversion recovery GE-EPI. Medical Physics. 2005; 32(4):1083–1093. [PubMed: 15895593]
29. Young JD, Dyar O, Xiong L, Howell S. Methaemoglobin production in normal adults inhaling low concentrations of nitric oxide. Intensive Care Med. 1994; 20(8):581–584. [PubMed: 7706572]
30. Gladwin MT, Schechter AN, Shelhamer JH, Pannell LK, Conway DA, Hrinczenko BW, Nichols JS, Pease-Fye ME, Noguchi CT, Rodgers GP, Ognibene FP. Inhaled nitric oxide augments nitric oxide transport on sickle cell hemoglobin without affecting oxygen affinity. J Clin Invest. 1999; 104(7):937–945. [PubMed: 10510334]
31. Siesjo BK. Cerebral-Circulation and Metabolism. Journal of Neurosurgery. 1984; 60(5):883–908. [PubMed: 6425463]
32. Chanarin, I.; Brozovic, M.; Tidmarsh, E.; Waters, D. Blood and its disease. New York: Churchill Livingstone; 1984.

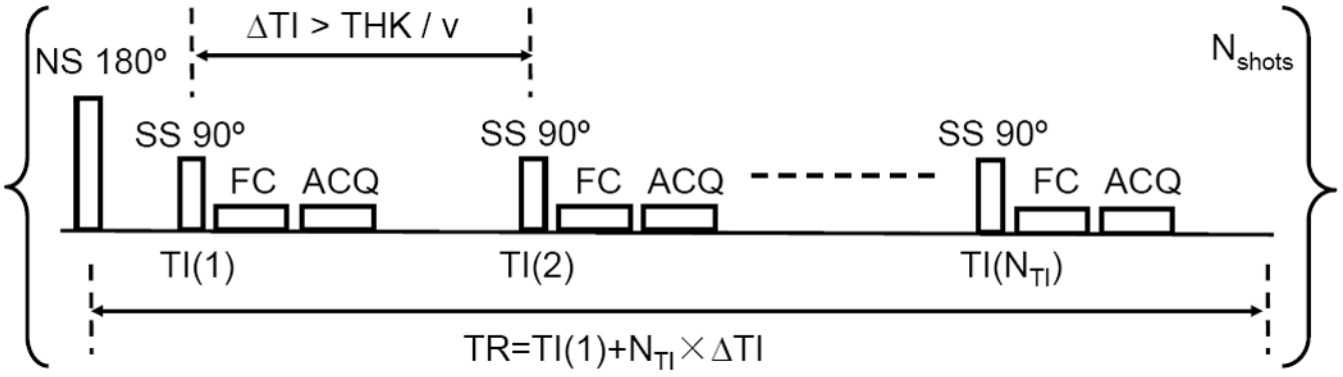

Fig. 1. Pulse sequence diagram for measuring T_1 of flowing blood

Following a non-selective (NS) 180° inversion pulse, a series of N_{TI} slice-selective (SS) 90° excitation pulses with short time intervals (ΔTI) are applied within one TR to sample the inversion recovery curve. THK = slice thickness; v = blood velocity; TI(1): initial TI value; FC: Flow Compensation gradients; ACQ: acquisition using segmented EPI readout train. It takes N_{shots} times to obtain the full *k*-space of each image at different TIs.

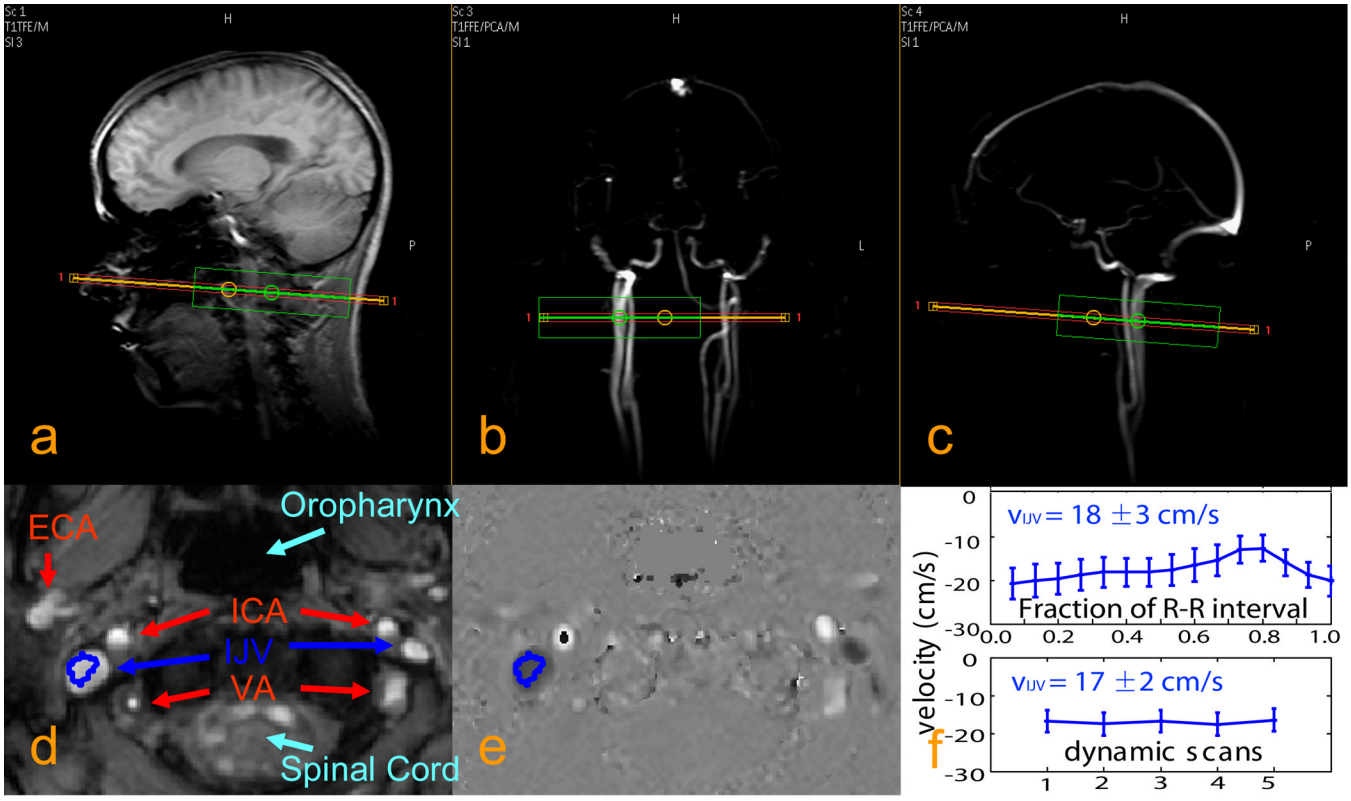

Fig. 2. Typical localizer images and blood velocity measurements for the internal jugular veins (IJVs)

a: anatomical scout image. b, c: angiographic scout images obtained using phase contrast MRA. The orange rectangle indicates the imaging slice for blood velocity measurements chosen perpendicular to the IJV. The green box is the localized shimming box (linear shims only). d: anatomical image of the selected slice, showing IJVs, internal carotid arteries (ICAs), external carotid arteries (ECAs), and vertebral arteries (Vas). e: quantitative velocity map (units of cm/s) for the selected slice. f: velocities measured with PPU triggering (top) and without triggering (bottom) for one of the healthy adult volunteers, showing good estimate of the average velocity with dynamic scans (bottom) even with some pulsatile flow (top) in IJV.

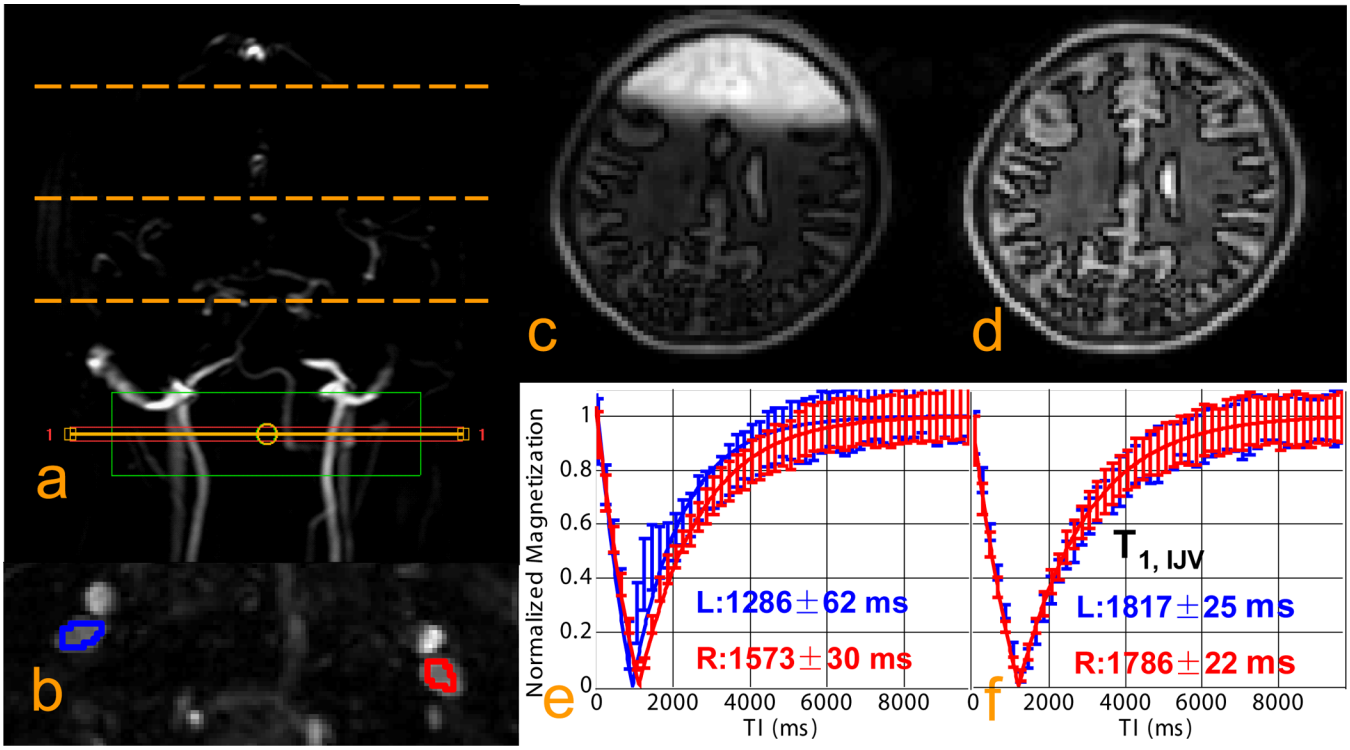

Fig. 3. Examination of non-selective inversion under different shimming conditions

a: positioning of the imaging slice for blood T_1 measurement (solid orange line and red box) and positioning of the imaging slices used to examine inversion quality for the top, middle, and bottom of the brain (dashed orange lines). The green box is the local shimming box covering both IJVs; b: ROI location for T_1 measurements from both IJVs; c, d: Inversion recovery images from the middle of the brain acquired at TI = 600 ms when using local 1^{st}/2^{nd} order shims (c) and when using local 1^{st} order shim only (d); e, f: inversion recovery curves from the two ROIs with fitted T_1s obtained with local 1^{st}/2^{nd} order shims (e) and with local 1^{st} order shim only (f). This shows the need for global shimming to allow proper whole-volume NS inversion.

Table 1

Variation of blood T_1 measurements depending on TR and slice thickness (n = 6)

	Blood T_1 (ms) mean ± sd		
	TR = 5 s	**TR = 7.5 s**	**TR = 10 s**
THK = 5 mm	1900 ± 100	1841 ± 104	1827 ± 109
THK = 10 mm	1891 ± 137	1831 ± 111	1800 ± 92

Table 2

Measured blood T_1 values from the internal jugular veins of 24 adult subjects*.

subject	$T_{1,\,IJV}$ (ms)	subject	$T_{1,\,IJV}$ (ms)
female:1	1919±32	male:1	1710±17
2	1983±29	2	1725±13
3	1841±31	3	1784±22
4	1911±18	4	1712±24
5	1913±16	5	1627±12
6	1980±24	6	1829±16
7	1819±21	7	1793±31
8	2019±52	8	1856±29
9	1970±25	9	1948±61
10	1896±30	10	1708±32
11	1928±35	11	1799±20
12	1906±20	12	1872±35
mean ± sd:	**1924 ± 58**	**mean ± sd:**	**1780 ± 89**
female and male data combined			
mean ± sd:	**1852 ± 104**		

*The standard errors of the fitted $T_{1,\,IJV}$ are shown as the uncertainty of the results for each individual.

Table 3

Measured blood T_1 values from 10 sickle cell patients and 8 sibling controls*.

Sickle Cell Patients					
subject	**Hct (%)**	**$T_{1,\,IJV}$ (ms)**	**subject**	**Hct (%)**	**$T_{1,\,IJV}$ (ms)**
female:1	24.4	1855±25	male:1	28.5	1886±48
2	16.6	1908±23	2	21.8	1858±40
3	24.3	1943±18	3	21.3	1909±13
4	26.3	1804±22	4	23.1	2064±30
5	25.1	2039±61	5	22.6	1975±30
mean ± sd:	**23.3 ± 3.9**	**1910 ± 89**	**mean ± sd:**	**23.5 ± 2.9**	**1938 ± 82**
Sibling Controls					
subject	**Hct (%)**	**$T_{1,\,IJV}$ (ms)**	**subject**	**Hct (%)**	**$T_{1,\,IJV}$ (ms)**
female:1	39.1	1949±20	male:1	34.8	1843±21
2	35.9	1972±18	2	41.4	1763±25
3	35.9	1934±34	3	42.4	1862±26
4	36.2	2089±30	4	42.4	1924±40
mean ± sd:	**36.8 ± 1.6**	**1986 ± 70**	**mean ± sd:**	**40.3 ± 3.7**	**1848 ± 66**

*The standard errors of the fitted $T_{1,\,IJV}$ are shown as the uncertainty of the results for each individual.